EXAMINATION OF GEARBOX CRACKS USING TIME-FREQUENCY DISTRIBUTIONS

H. Oehlmann, D. Brie, V. Begotto and M. Tomczak
CRAN CNRS URA 821
B.P. 239, F-54506 Vandoeuvre Cedex, France
E-Mail : oehlmann@cran.u-nancy.fr

ABSTRACT

Nonstationary gearbox vibration signals are analysed using a time-frequency (TF) representation which is chosen with respect to its interpretability. With its help, a crack transient is examined in detail and decomposed into three physical parts. Following this analysis, a time-domain signal is synthesized. Its good phase fitting proves on one hand, the validity of the analysis and on the other hand, the good accuracy of the TF representation chosen.

1. INTRODUCTION

The understanding of the way faults are developing in gearboxes is important for their design and maintenance. The gearbox vibration signals give an indication of physical processes in the gearbox, eventually with transient phenomena due to cracks meshing. These signals are multi-component signals that include tooth meshing (with or without crack), gearbox resonance vibrations, and system and sensor transmission characteristics. Time-frequency (TF) representations are considered to analyse those signals with the aim of isolating the different physical processes.
The representation of a signal in the TF plane found interesting applications in physics (quantum mechanics) and engineering [1-3]. Within this framework, the analysis of mechanical vibration signals is of special interest [4-7].
In this paper, a TF analysing method is presented and applied to a gearbox vibration signal. The operating conditions and the recorded signal are first presented. Next, the choice of the TF representation is discussed under the scope of leading to an easy physical interpretation of the underlying phenomena. Afterwards, the TF representation of one crack signal is analysed and physically interpreted. This leads to a time domain crack signal model including the main structures of the TF representation. The accuracy of the corresponding synthesized signal validates our analysis. Finally, conclusions and perspectives are given.

2. THE GEARBOX SIGNAL

We are using a car gearbox, driven with two asynchronous motors at 4500 rpm with a break-momentum of 80 Nm, running in the first gear and using a tooth-ratio of 12/41. On the driven helical wheel is a small crack.
The vibration of the whole box is taken with an accelerometer low-pass filtered at 10 kHz. The signal is sampled with a fixed rate of 28 kHz.

To extract the effects caused by the damaged wheel, 33 shaft rotation signals are averaged synchronously to that wheel.

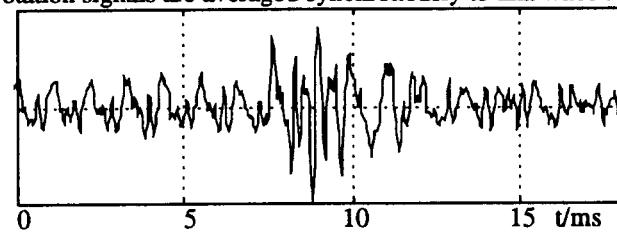

figure 1 : Vibration signal

Figure 1 shows 23 teeth meshings with one crack in the middle. This signal is nonstationary over the crack transient.

3. CHOICE OF A TF DISTRIBUTION

Frequency is only defined for an infinite time-axis. Nevertheless, a time located frequency concept enables a more detailed analysis of transient signals and leads to a physically meaningful interpretation of underlying phenomena. Regarding energy, we wish the localization of energy in time and frequency to result in a TF distribution.
This approach seems to be appropriate for gearbox vibration signals, because the shocks involved by a crack cause an increase of mechanical system energy, leading to a rising frequency and amplitude (signal energy) of the signal. So we wish a method to extract the signal energy as a function of time and frequency (as defined by the instantaneous frequency law or others).
One approach of such distributions is Cohen's Class [3,7] : the distribution $P_{(t,f)}$ of the signal $s_{(t)}$ is the two-dimensional Fourier-transform of the ambiguity function $A_{(\tau,\theta)}$ of the signal weighted by a function called the kernel $\Theta_{(\tau,\theta)}$:

$$P_{(t,f)} = FT^{2D}\left\{\Theta_{(\tau,\theta)} A_{(\tau,\theta)}\right\}.$$

The ambiguity function compares a signal with itself shifted in time and frequency :

$$A_{(\tau,\theta)} = \int_{t=-\infty}^{\infty} s_{(t+\frac{\tau}{2})} s^{*}_{(t-\frac{\tau}{2})} e^{j\theta t} dt.$$

Choosing the kernel equal to one yields the well known Wigner distribution [1]. Supposing a multi-component signal, the ambiguity function consists of auto-components due to the product of one component of the signal, and cross-components created by the multiplication of different signal components. The cross-components cause interference structures in the TF distribution which highly complicate the physical interpretation.

0-7803-2431-5/95 $4.00

Supposing that different components are separated by a certain distance in the TF plane, their cross-components will have exactly that distance from the origin in the ambiguity plane. They are separated from the auto-components which are located around the origin . Figure 2 shows an example illustrating the way from a test signal consisting in two gaussians to its TF representation.

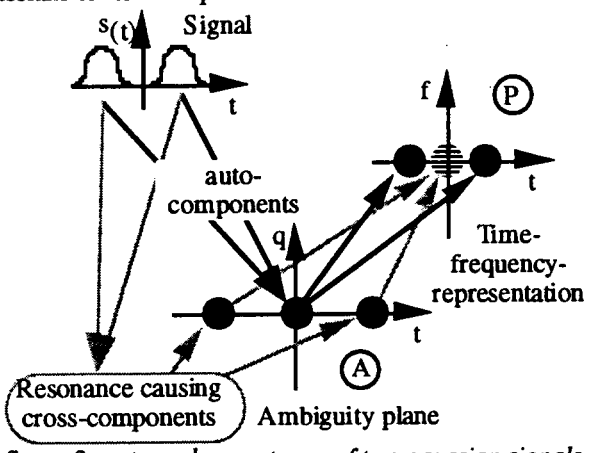

figure 2: auto and cross-terms of two gaussian signals

Those cross-terms may be suppressed with a proper choice of the kernel. Typically, low-pass formed kernels suppress cross-terms, but too small a kernel corrupts the auto-components.

Among the existing methods using this technique [7-9] the optimal design of the kernel [10] seems to be the most interesting one : the kernel is evaluated in dependence of the signal represented by its ambiguity function. We try to find the low-pass kernel $\Phi_{(\tau,\theta)}$ which covers the maximum of energy of the ambiguity plane by holding a fixed kernel volume :

$$\max_{\Phi} \int_{-\infty}^{\infty}\int_{-\infty}^{\infty} \left|A_{(\tau,\theta)}\Phi_{(\tau,\theta)}\right|^2 d\theta d\tau$$

with the constraints : $\Phi_{(0,0)} = 0$, $\Phi_{(\tau,\theta)}$ is radially nonincreasing (low-pass) and the kernel volume is smaller than a given value V.

This method results in very sharp auto-components, independently of their time-frequency orientation, with interference structures strongly reduced, which leads to an easier interpretation. In addition, the representation is very local in time and frequency because of the low-pass kernel.

When using this method the kernel volume V has to be chosen. Successive trials with our signals have shown that a fixed value of V=0.5% of the maximum volume of the discrete ambiguity plane, which covers the main signal energy, gives good results. Even if the representations change with the kernel volume chosen, the main structures are included for the whole reasonable interval.

4. ANALYSIS OF THE SIGNAL

Figure 4 shows a zoom of the TF representation calculated. The full size would be 43 ms (1 rotation) x 14 kHz.

The meshing frequency and its harmonics are visible at 902 Hz and multiples. The structure representing a shock is an energy concentration over a time interval of about 4 teeth meshings.

In the following, we discuss the time evaluation of the signal in detail. The time instants are marked in the TF representation on figure 4 and illustrated on figure 3, which shows, how a cracked tooth meshes over in one rotation[11].

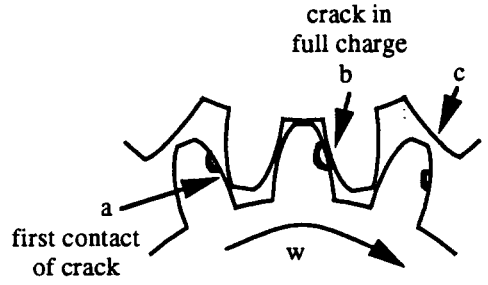

figure 3 : crack meshing

(a) First contact of the crack

The energy spot at time instant (a) represents the first contact of the crack. Only a relatively low force is taken by the tooth with failure.

(b) Maximum load on the crack

At this time, the peek representing the tooth meshing is delayed in time due to missing material in the crack. The following shock, due to the full loading of the tooth, implies an increase of energy of the mechanical system which results in an increased frequency value of about 2400 Hz and an amplitude of three times the usual. This effect starts already before the maximum (b) at a higher frequency of about 3100 Hz.

Then, the supplementary energy starts to dissipate. The frequency of the crack phenomenon decreases linearly with time and the amplitude falls too. This dissipation is caused by the energy absorption of the oil in the box and the whole mechanical system. This effect characterizes mainly the crack meshing making it the central point of section 5.

(c) Third contact of the crack

In this position, the cracked tooth is meshed with a small amount of load, which causes a small energy spot, similar to that of position (a).

(d) Normal state

Two teeth after the main shock, all supplementary energy has been dissipated and the normal tooth meshing takes place.

The components that have just been evidenced are used in the next section to synthesize a meaningful time-domain model.

5. CRACK SIGNAL MODEL

In an attempt to validate the analysis of the previous section by proving that the major components found do exist, we try to synthesize a simplified but accurate time domain

model including the typical features of a crack-class. It may also be useful in fast detection and classification procedures. This is achieved by first, the synthesis of the time-signal and second, the comparison of the actual and the synthesized signal and their TF-representations.

The reconstruction of a signal from a TF representation is a delicate problem[7]. A simplified approach was adopted to obtain a time-domain model using the instantaneous frequency law. We suppose that each physical components found in the TF plane may be described by a straight line with variable amplitude. Its time signal is following the instantaneous frequency law :

$$c_{(t)} = A_{(t)} \cos(2\pi \underbrace{\left(f_0 + \frac{\Delta f}{2} t\right)}_{f_{(t)\ \text{linear}}} t + \varphi_0)$$

The final model is the sum of lines :

$$\hat{s}_{(t)} = \sum_i A_{i(t)} \cos\left(2\pi (f_{0i} + \frac{\Delta f_i}{2} t) t + \varphi_{0i}\right).$$

with the following parameter evaluation :

- Number of lines i : we considered four lines : two meshing frequencies (902 Hz, 1805 Hz), main crack line (3718 Hz 79 ms - 738 Hz 108 ms) and the line joining the two power spots at 1121 Hz.
- Line position $f_{0i}, \Delta f_i$: Approximating the maxima chain by straight lines is valid because only one point doesn't fit exactly.
- Phase φ_{0i} : the phases are estimated by correlation or non-linear optimization of the quadratic error.
- Amplitude $A_{i(t)}$: a good method would be to integrate the square-root of the TF representation in a region around each line point. Those integrals are approximated by the value of the square root of the TF representation on the four lines considered scaled by individual constant factors α_i, which are found by optimization of the quadratic error : $A_{i(t)} = \alpha_i \sqrt{P_{(t,f_{(t)})}}$.

The resulting model is compared with the actual signal in the lower part of figure 5. The upper part shows the TF representation of the model. For these results the actual signal was low pass filtered at 4006 Hz to reduce high frequency components not included in the model.

Looking at the reconstruction in detail it appears that the amplitude estimation is poor. This is due to the rough approximation of the integral. However, the synthesized and actual signals are well in phase over the transient part. Thus, the frequency variation of the main crack line is well described by the linear chirp. Moreover the TF representations are very close, even in maxima and cross-terms.

6. CONCLUSION

TF representations of gearbox-vibration signals show gear-failures in a characteristic way, representing the process of increasing system energy. They allow a physical interpretation leading to a better understanding of the cracking evolution. Taking into account the components given by the physical analysis, leads to a time domain model consisting of linear chirps.

The fact that this signal model has nearly identical frequency variations as the actual signal validates our physical analysis (choice of components) and the good accuracy of the TF representation.

Our future works will be oriented toward the classification of gearbox faults like cracks, bearing failures, wearings or shaft misalignments, with the use of TF representation based models. This opens the perspective to an early warning system for gearbox failures, preventing abrupt crashes and expensive maintenance.

REFERENCES

[1] E. P. Wigner : "On the quantum correction for thermodynamic equilibrium", Phys. Rev., Vol. 40, 1932, pp. 749-759.

[2] J. Ville : "Théorie et applications de la notion de signal analytique", câbles et transmissions, 2ème A., No. 1, 1948, pp. 61-74.

[3] L. Cohen : "Generalised phase-space distribution functions", J. Math. Phys., Vol. 7, No. 5, 1966, pp. 781-786.

[4] B. D. Forrester : "Analysis of gear vibration in the time-frequency domain", Proceedings of the 44th Meeting of the Mechanical Failures Prevention Group of the Vibration Institute, Virginia Beach, Virginia, 3-5. April 1990, pp. 225-234.

[5] B. Boashash, P. O'Shea : "A methodology for detection and classification of some underwater acoustic signals using time-frequency analysis techniques", IEEE Trans. on Acoust., Speech and Signal Proc., Vol. 38, No. 11, 1990, pp. 1829-1841.

[6] W. J. Wang, P. D. McFadden : "Early detection of gear failure by vibration analysis - I. Calculation of the time-frequency distribution", Mechanical Systems and Signal Processing, Vol. 7, No. 3, 1993, pp. 193-`203

[7] P. Flandrin : "Temps-fréquence", Editions Hermès, Paris, 1993, ISBN 2-86601-387-5

[8] H. I. Choi, W. J. Williams : "Improved time-frequency representation of multicomponent signals using exponential kernels", IEEE Trans. on Acoust., Speech and Signal Proc., Vol. 34, No. 6, 1989, pp. 862-871.

[9] Y. Zhao, L. E. Atlas, R. J. Marks : "The use of cone-shape kernels for generalized time-frequency representations of nonstationary signals", IEEE Trans. on Acoust., Speech and Signal Proc., Vol. 38, July 1990, pp. 1084-1091.

[10] R. G. Baraniuk, D. L. Jones : "A signal-dependent time-frequency representation : optimal kernel design", IEEE Trans. on Signal Processing, Vol. 41, No. 4, 1993, pp. 1595-1602.

[11] L. Faure : "Aspect des dentures d'engrenage après fonctionnement", Centre d'Etudes Techniques des Industries Mécaniques, ISBN 2-85400-157-5

[12] G. F. Boudreaux-Bartels, T. W. Parks : "Time-varying filtering and signal estimation using Wigner distribution synthesis techniques", IEEE Trans. on Acoust., Speech and Signal Proc., Vol. 34, June 1986, pp. 442-451.

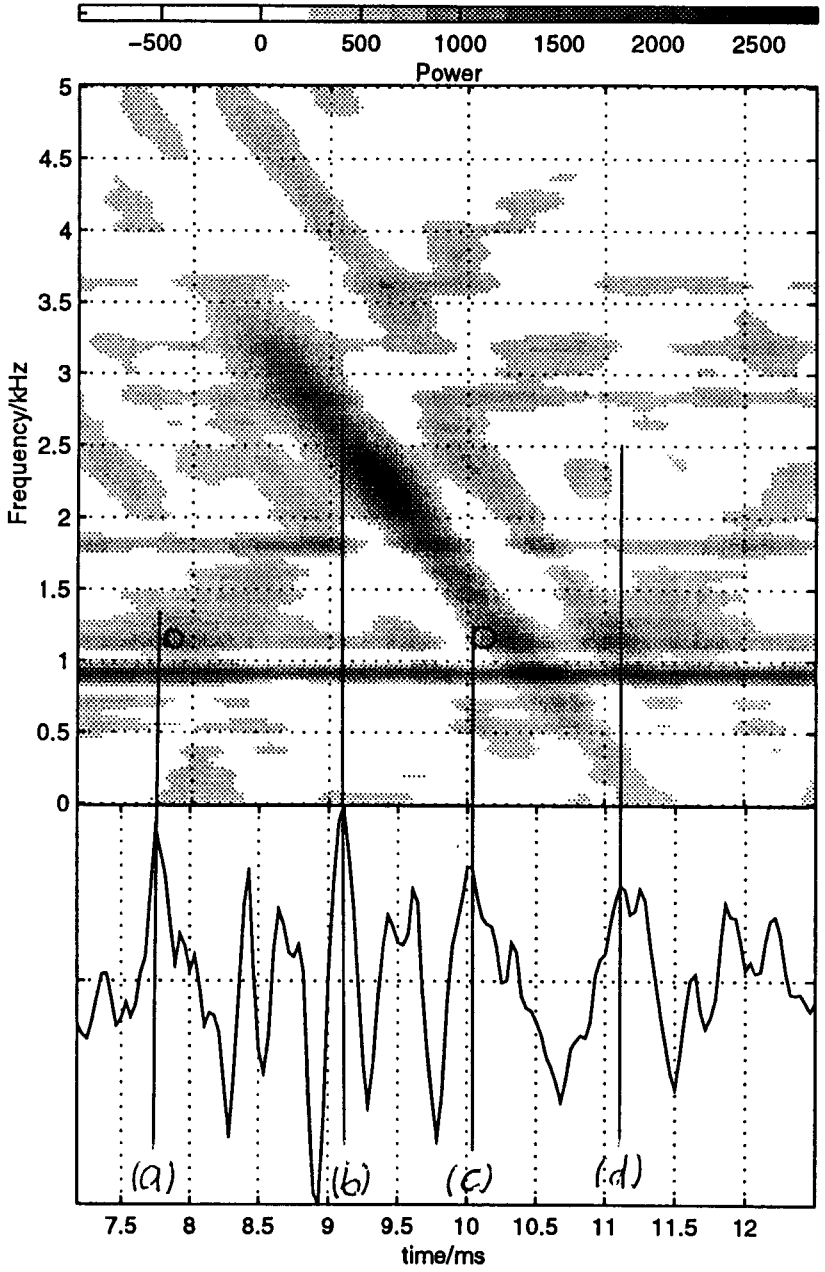

Figure 4 : actual signal and its TF representation

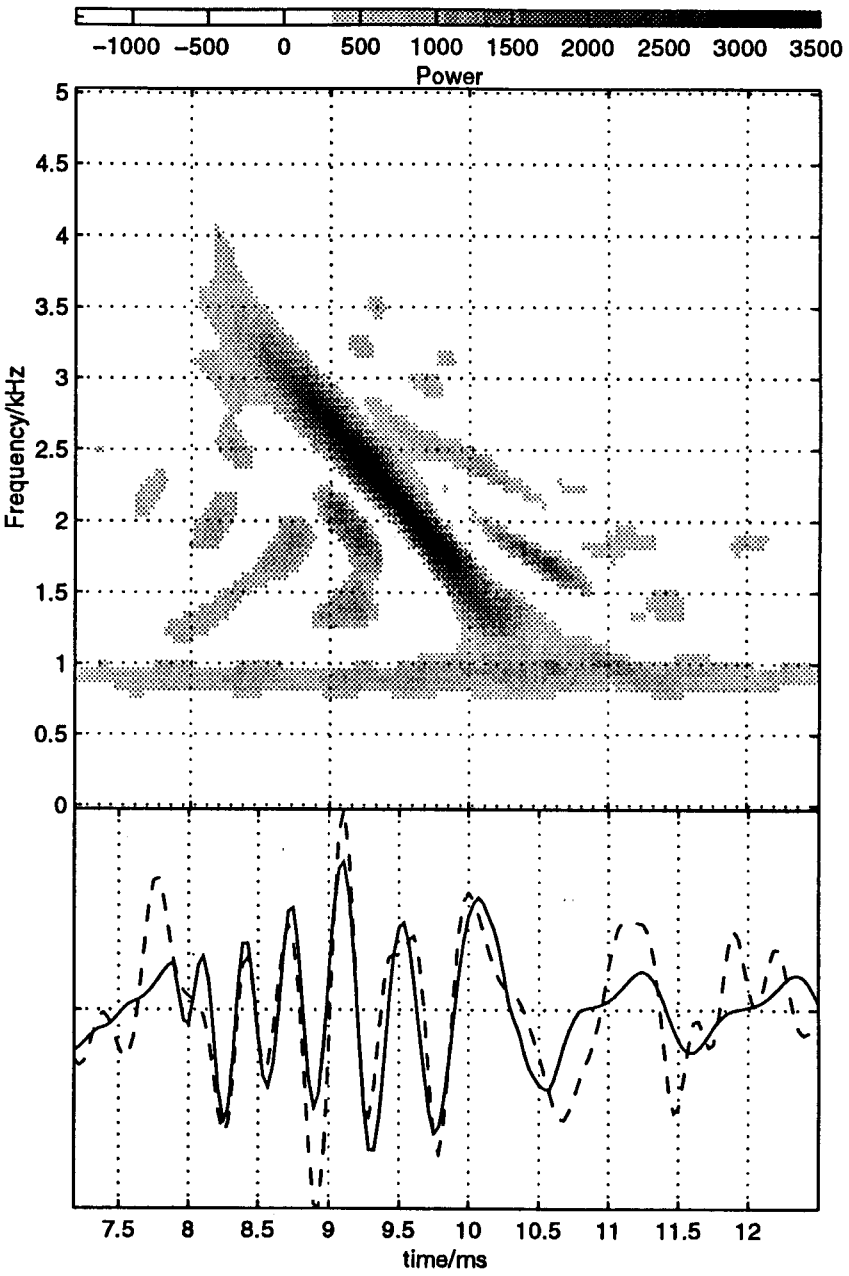

Figure 5 bottom : synthesized signal (dashed) and filtered actual signal (solid)
up : TF representation of synthesized signal